Polytechnic Journal. 2022. 12(1): 40-54
ISSN: 2313-5727
http://journals.epu.edu.iq/index.php/polytechnic

POLYTECHNIC JOURNAL

RESEARCH ARTICLE

Influence of time-dependent corrosion on strength and ductility of reinforcing steel bars exposed to natural and aggressive environments

Ghafur H. Ahmed*

Department of Highway and Bridge Engineering, Technical Engineering College, Erbil Polytechnic University, Erbil, Kurdistan Region, Iraq

***Corresponding author:** Ghafur H. Ahmed, Department of Highway and Bridge Engineering, Technical Engineering College, Erbil Polytechnic University, Erbil, Kurdistan Region, Iraq. **E-mail:** ghafur.ahmed@epu.edu.iq

Received: 12 February 2022
Accepted: 10 April 2022
Published: 11 August 2022

DOI
10.25156/ptj.v12n1y2022.pp40-54

ABSTRACT

The reinforcement corrosion is a major and most frequent reason of degradation for reinforced-concrete (RC) structures throughout the world, leading to their premature deterioration before design life was attained. Corrosion weakens the mechanical properties of rebar by ingress of aggressive ions due to various environments. In this study, a total of 99 specimens with six different diameters were tested, for three exposure periods, and six different environments, to assess the influence of corrosion on mechanical properties of reinforcing bars. Degradation relationships of strength and ductility with exposure period and rebar diameter, were analyzed, and three equations were proposed to formulate the relations. It was found that, the ultimate strength of 8.6% of the corroded bars falls below the original yield strength; after 5 years of exposure in natural atmosphere, reduction in mechanical properties was insignificant; a detergent solution environment could cause the strength loss of 24.8%.

Keywords: corrosion; steel bar; mechanical properties; pitting corrosion; fracture strain

INTRODUCTION

Corrosion of reinforcing steel bars is one of the most frequent and significant types of deterioration mechanisms in existing reinforced concrete structures. Corrosion leads to expansive pressure on the surrounding concrete that causes internal cracking and, eventually, spalling and delamination, even collapse of the structures. It is worth noting that extensive cracking in concrete can be observed even when structure's service life is within 10 years (Wu et al. 2019; Zhang et al. 2020). Corrosion is commonly perceived as one of the most detrimental factors causing degradation of serviceability and durability of RC structures, and it became a global problem over the past decades. Direct and indirect costs of maintenance and repair are very high. The statistics data indicated that the mean mass corrosion rate for natural exposure reached to 0.5% per year. Since corrosive action manifests itself in objects from building structures, constructions and bridges, transportation systems household materials and appliances, the economic damage is huge. For instance, according to investigations, the annual total direct corrosion losses in the USA in 26 sectors of industry are about 276B USD. Therefore, it is of great significance to cast sight on the corrosion-induced problems (Babutskii, 2010; Miao et al. 2019; Bidi et al. 2020). The rate of change in rebar mechanical properties is depending on the corrosion duration, bar size as well as the exposure environments. The yield and ultimate stresses of the naturally and artificial corroded bars are similar, while the ultimate strain of the naturally corroded bars is smaller than that artificially corroded (Fernandez et al. 2015; Diaz et al. 2020). Although many studies have been conducted; however, research on effects of corrosion on mechanical properties of tensile reinforcements still lacks clarity. Studies considering the mechanical properties of naturally corroded rebar obtained from real structures exposed to aggressive environments might include more scattered results, since the corroded bar results were calibrated with those considered un-corroded from the same

structures, however, the second might had a degree of corrosion and they were stressed already. Most studies analyzed time-dependent corrosion in accelerated tests, i.e. establishing the theoretical and empirical models of corrosion based on the current density. However, these models have no consistent conclusion yet, due to various influencing factors considered in different tests. A little research explored the influence of saturated deteriorated concrete exposed to aggressive environments due to low quality of concrete or age degradations. The influence of rebar diameter on the corrosion propagation had rarely been studied (Finozzi et al. 2018; Balestra et al. 2019).

This study presented the experimental results of 99 corroded and un-corroded reinforcing bars, exposed to six naturally possible environments with different degree of aggressiveness. The corrosion period was 1, 3 and 5 years, and the environments were: natural atmosphere, soil buried, and immersion of specimens in ground water, salty water, rain water and a detergent solution, from which, the last two conditions had rarely been studied. The relations of, the exposure period and environments with the bar diameter (8, 10, 12, 16, 20 and 25 mm) were presented for the mass loss, strength and ductility, from which interesting results were revealed. Deterioration equations for corroded rebar mechanical properties and the reduction coefficients were proposed that can be usefully adopted in analytical and numerical structural applications.

2. MATERIALS AND METHODS

2.1. Properties of the un-corroded reinforcing bars

Deformed reinforcing steel bars were used with six different diameters including 8, 10, 12, 16, 20 and 25 mm. The tensile properties of the bars and the nominal parameters such as diameter, area, mass, deformation and rib dimensions were presented in Table 1. The tensile properties (yield strength, ultimate strength, and elongation) tested according to ASTM 370 (2019) and evaluated to ASTM A615 (2009). The dimensions and the mechanical properties of the rebar are averages of 3 specimens for each diameter.

2.2. Test environments and exposure conditions

To investigate the influence of different possible environments in corrosion of reinforcing steel bars, the total exposure of six different environments have been studied. The teste environments were: (i) exposure to natural atmosphere (AT), in which the bare reinforcing bars were exposed to natural weather conditions for 1, 3 and 5 years (Fig.1). Three sets of the samples were exposed to natural environmental thermal daily and seasonal temperature and humidity of Erbil city in Kurdistan Region-Iraq. The rebar was not in contact with any surface and they were rotated periodically. The average long-term weather information and climate records of the city are illustrated in Table 2. (ii) Specimens buried in soil (SL), for this group the bare rebar was buried in soil to a depth of 100 mm, as shown in Fig.1b. The characteristics and chemical analysis of the soil are presented in Table 3. The humidity, and water content and the temperature inside the soil containers were depending on the seasonal climate changes, rain infiltration and ambient temperature. The soil containers were drained to prevent accumulation of water during rainfall. As presented in Table 3, the soil was a highway subbase material and not having characteristics of water retention. Furthermore, the pH verified is associated with the presence of calcium carbonate (pH = 9.9), contributing to an alkaline environment, which is compatible with alkaline behavior of cement, noting the pH value of Portland

Table 1 Dimensions, deformations and mechanical properties of the reinforcing bars compared with ASTM A615 limitations

Bar des. No.	nominal mass (kg/m)	nominal dimensions		deformation requirements (mm)			Yield strength (MPa)		Tensile strength (MPa)		Elongation (%)		Grade
		dia. (mm)	section area (mm^2)	max. avg. spacing	min. avg. height	max. gap	test	sp.	test	sp.	test	sp.	
08	0.399	8.0	50.8	4.60	0.69	1.20	675.4	550	782.8	725	11.7	7	G550
10	0.595	9.8	75.8	6.32	0.50	1.46	689.8	550	820.3	725	10.9	7	G550
12	0.850	11.7	108.3	7.66	0.69	1.60	617.6	550	742.2	725	17.2	7	G550
16	1.573	16.1	203.6	9.66	0.94	2.50	447.5	420	654.0	620	17.7	9	G420
20	2.393	19.7	304.8	12.71	1.17	2.94	570.3	520	717.8	690	16.8	7	G520
25	3.963	25.4	504.8	15.64	1.37	3.24	552.7	420	667.1	620	17.6	8	G420

cement is 11 (Ahmed, 2021). (iii) Specimens immersed in ground water (GW), three sets of six bars were immersed in ground water by using 650 mm deep plastic buckets (pails), as shown in Fig.1c. The buckets were laid in the room temperature which fluctuates freely with the seasonal weather changes. The ground water was obtained in a well and tested for chemical properties shown in Table 4. (iv) Specimens submerged in rain water (RN), to verify if the rainfall is causing an aggressive corrosion to the bare reinforcing bars, three sets of 10, 12 and 16 mm bars were submerged in collected rain water, for 1, 3 and five years. (v) Specimens submerged in salty water (SW), the salty water was prepared by dissolving a ratio of 100 g of NaCl in each liter of water, which produces approximately three times a chloride concentration exists in seawater (3.5%). Three sets of specimens were submerged in the salty-water for 1, 3 and 5 years. The buckets were put in shade at the room temperature that varied according to seasonal weather changes. The concentration of NaCl solution of 3.5% was used by Tittarelli et al. (2018), 5% by Uthaman et al. (2019) and 12.5% by Gao et al. (2019). (vi) Specimens immersed in a detergent solution (DS), to investigate the influence of detergents on corrosion of rebar, a solution was prepared by dissolving 1.0 kg of Ariel detergent powder in 40 liters of water, i.e. 25 g/L. Three sets of specimens (10, 12, and 16 mm bars) were submerged in the detergent solution bucket for 1, 3 and 5 years. The composition of the solution is presented in Table 4.

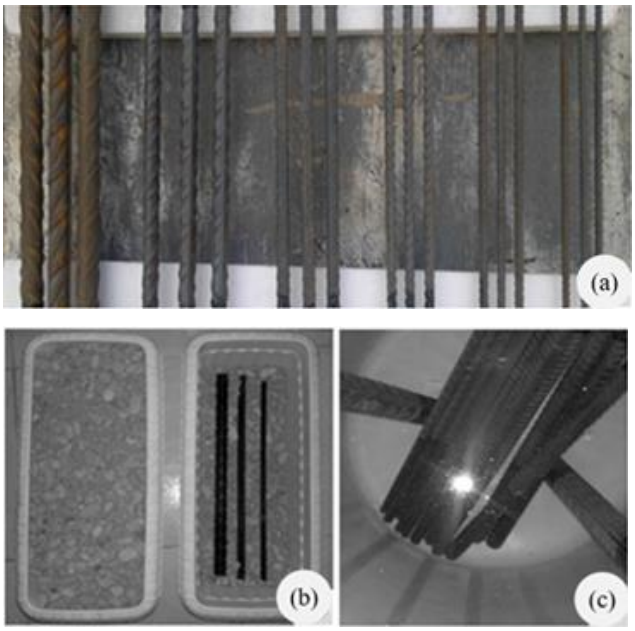

Fig.1. (a) three sets of rebar exposed to natural atmosphere (b) Reinforcing bars buried in the soil, and (c) buckets used for immersing bars

Table 2 Climate information for specimens exposed directly to the atmosphere

Climate/Month	Jan	Feb	Mar	Apr	May	Jun	Jul	Aug	Sep	Oct	Nov	Dec
Avg. high temperature (°C)	12.4	14.2	18.1	24.0	31.5	38.1	42.0	41.9	37.9	30.7	21.2	14.4
Avg. low temperature (°C)	2.4	3.6	6.7	11.1	16.7	21.4	24.9	24.4	20.1	14.5	8.9	3.9
Avg. humidity (%)	74.5	70.0	65.0	58.5	41.5	28.5	25.0	27.5	30.5	43.5	60.5	75.5
Avg. rainfall (mm)	111	97	89	69	26	00	00	00	00	12	56	80
Avg. daylight (hr.)	10.0	10.9	12.0	13.1	14.1	14.6	14.3	13.5	12.4	11.3	10.3	9.7

Table 3 Sieve analysis, classification & composition, and chemical analysis of the soil of the soil

Sieve analysis		Classification and composition		Chemical analysis	
Sieve size	Passing (%)	Test	Results	Test	Test results
25	100	Liquid limit	22	TSS (%)	0.042
19	83	Plasticity index	NPI	pH	7.69
9.50	48	Coefficient of uniformity Cc	10.20	CaCO3 (%)	7.2
4.75	27	Coefficient of curvature Cu	45.17	Chloride Cl- (%)	0.011
2.36	21	Gravel (%)	73	Sulfate SO3 (%)	0.086
2.00	19	Sand (%)	21	Na2O (%)	0.008
0.425	12	Fines (%)	6		
0.300	10	Classification (AASHTO)	A-1-a, (0)		
0.075	6	Classification (USCS)	GP-GM		

Table 4 Chemical analysis of different liquids representing different environment

Test condition	TDS (%)	pH	Chloride Cl- (%)	Carbonate CO_3^{-2} (%)	Bi-Carbonate HCO_3- (%)	Sulfate SO_4^{-2} (%)	Solids (%)	Organic M. (%)	Unit weight @ 4°C
GW	0.0110	7.3	0.005	Nil	0.009	0.004	0.62	0.020	1.0070
RN	0.0045	6.7	0.004	Nil	0.008	0.002	0.13	Nil	1.0002
SW	8.6000	7.5	4.680	Nil	Nil	0.100	1.02	0.082	1.0860
DS	0.6500	9.8	0.004	0.060	0.080	0.160	0.20	0.011	1.0065

2.3. Testing and measurements

At the end of each exposure periods, the specimens were removed from soil or buckets, and the corrosion products that adhered to the surface of the bars were completely cleared (Fig.2a). It is worth noting that the corrosion products on the surface of corroded reinforcements should be removed before measuring the corrosion rates, which allowing a better visualization of pits present in the specimens and accurate measurements of the mass loss. Afterward, a fine search was performed, seeking for the type of corrosion (uniform or pits) and the residual diameter of rebar. Finally, the rebar was tested for mechanical properties using the machine shown in Fig.2b with the capacity of 600 kN, and 0.1 kN accuracy.

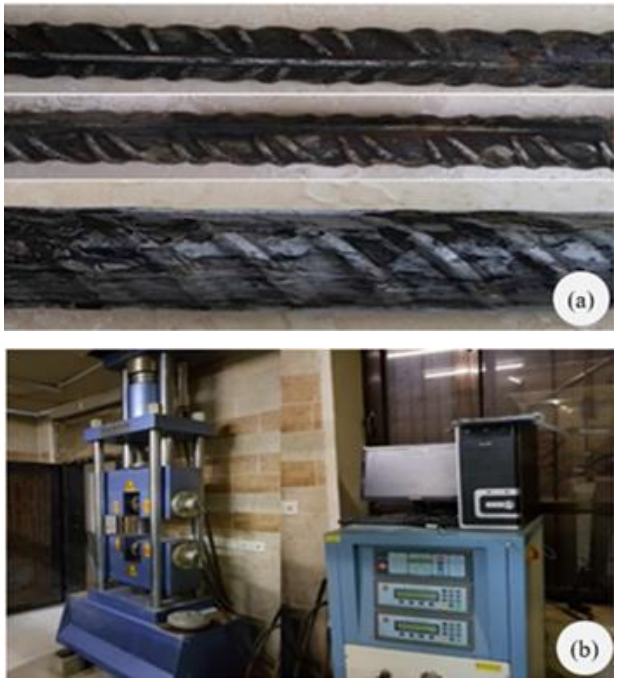

Fig.2. (a) Cleaned specimens from rust and corrosion products, (b) The machine used for tensile testing.

3. RESULTS AND DISCUSSIONS

In this section, the test results of the reduced mechanical properties were presented and discussed, also the evolution of the corrosion and growth of the rust layer were analyzed. Table 5 is illustrating the results of the rebar exposed to different environmental conditions for 1, 3 and 5 years. The data include, nominal bar diameter, reduced area, elastic limit stress, tensile strength, and strain corresponding to the failure load.

3.1 Residual area and the mass loss

In this work, the average mass-corrosion rates of reinforcement under the corresponding exposure condition were calculated according to Eq.1. It should be noted that the residual cross-section of the corroded reinforcement was calculated by the residual mass divided the density of steel and the length of the corresponding specimen. So the residual section represents average value over the specimen length. As the effective strength values are calculated considering the corroded section, this parameter should be used for assessment of corroded structures, whereas nominal parameters should be used for un-corroded members.

The mass losses of all specimens according to the six mentioned environments are presented in Fig.3, that the same scale for the entire figures was intended to make comparison easier.

$$\Delta M(\%) = \frac{M_o - M_c}{M_o} * 100 \quad (1)$$

Where:

Table 5 Mechanical properties of un-corroded and corroded specimens in three different periods of exposure

S	Exp. Environ.	Dia.(mm)	Residual parameters after (t) years											
			Area (mm2)			Yield strength (MPa)			Ultimate strength(MPa)			Elongation (%)		
			1	3	5	1	3	5	1	3	5	1	3	5
1	AT	08	050.7	050.6	049.9	673.2	644.6	622.3	777.5	765.2	734.2	11.7	11.5	10.8
2		10	075.6	075.3	074.6	695.4	682.1	643.2	811.4	798.4	737.8	11.0	10.8	10.1
3		12	108.2	107.3	106.8	615.3	583.9	577.1	740.4	738.2	729.3	17.1	16.5	16.2
4		16	203.1	202.8	200.3	448.6	439.7	433.7	645.3	641.1	596.3	17.7	17.3	16.9
5		20	304.6	303.1	301.8	571.2	564.2	558.4	703.8	699.8	693.8	16.8	16.7	16.7
6		25	503.9	499.7	496.7	555.3	544.1	539.4	665.6	660.3	662.1	17.5	17.6	17.4
7	SL	08	050.2	049.2	047.4	642.1	576.6	542.6	722.9	673.1	649.0	11.4	10.7	10.3
8		10	075.1	073.6	070.7	660.9	610.7	581.2	768.3	725.4	699.1	10.7	10.3	09.7
9		12	107.4	104.9	102.3	595.8	580.3	542.8	712.1	702.0	671.0	16.7	15.4	14.1
10		16	201.8	199.6	194.9	437.5	426.2	405.8	633.1	627.3	600.0	17.3	16.5	15.7
11		20	301.4	297.6	291.7	565.1	547.9	531.2	709.2	686.8	668.6	16.2	16.1	15.8
12		25	499.8	494.2	482.3	543.6	528.2	512.8	649.6	621.8	616.2	17.5	16.9	16.2
13	GW	08	050.2	049.4	047.1	581.4	562.4	552.7	681.1	647.1	623.0	10.3	09.8	08.9
14		10	075.0	074.6	070.8	640.1	621.5	588.0	751.4	748.4	727.7	10.2	09.7	08.7
15		12	106.8	105.8	103.2	603.0	585.5	555.9	698.7	676.7	650.9	14.1	13.5	12.6
16		16	198.6	197.7	193.4	419.7	414.7	412.3	615.0	600.7	580.2	17.3	16.7	14.7
17		20	304.5	304.1	298.8	569.5	568.4	524.2	702.3	661.0	641.2	16.1	15.4	14.5
18		25	497.3	495.2	491.2	553.8	543.2	516.3	663.2	646.8	641.2	17.1	16.9	16.4
19	RN	10	074.1	073.1	071.8	654.2	629.8	601.9	789.4	736.6	707.1	9.9	09.1	08.2
20		12	105.6	104.4	103.1	589.4	556.1	548.9	708.6	688.7	658.4	15.9	14.8	14.4
21		16	198.4	197.7	193.7	428.3	423.4	418.3	621.4	621.4	613.4	16.8	15.3	13.7
22	SW	10	073.6	071.4	069.6	650.4	600.3	566.2	769.4	714.3	663.4	10.4	09.8	08.5
23		12	105.5	104.1	102.1	591.3	544.1	521.9	708.1	653.2	626.4	16.6	15.7	13.8
24		16	200.5	199.8	194.2	437.2	397.4	381.9	640.7	605.3	587.7	16.9	16.0	14.4
25	DS	10	072.2	070.1	068.1	648.6	598.6	567.3	767.7	706.2	616.9	10.2	08.8	08.2
26		12	104.1	102.1	098.5	601.2	569.3	522.9	701.0	662.1	595.8	16.7	14.3	12.6
27		16	197.4	194.8	189.4	440.0	419.3	411.5	625.5	576.9	533.7	17.4	15.9	14.1

ΔM = mass loss of the bars (%), M_o = the line density of un-corroded reinforcement (g/mm), Mc = the line density of corroded reinforcement (g/mm).

In case of the rebar exposed to natural environment, the mass loss of the entire bars was below 2% after even five years of exposure, and when comparing to other groups, the condition is not aggressive, and the corrosion was uniform. Uniform corrosion is as a type of attack that is more or less uniformly distributed over the entire exposed surface of a bar. The color of the rebar surface had changed to a reddish brown with dark brown spots (Fig.4a), and the corrosion product based on the rust color was $Fe(OH)_3$ with the relative volume of 4.2 compared to Fe (Wang et al. 2010). The maximum mass loss of one-year exposure was 0.26% for Ø10 mm specimen, whereas in five years Ø8 mm exhibited the maximum loss of 1.77%. Gao et al. (2019) mentioned that, the mean mass corrosion rate for natural exposure reached 0.5% per year, and the ratio is analogous with that recorded in this study. Further, regarding the corrosion types shown in Fig.4a, Diaz et al. (2020) stated that, the visual aspect of the rebar was that of un-corroded steel, with only a little rust-like color. However, the cross-section view in SEM image reveals the presence of apparently homogeneous oxides layer of about 28 μm thick with some cracks.

The soil used for rebar specimens to be buried in, was road subbase material, so it contained only 6% of fines, not like the clayey soils that has a high possibility of water retention, and thus the aggressiveness of the soil has reduced. The soil environment was alkaline based on its pH, and the carbonate content could help in acceleration of corrosion. For this group, corrosion products were: Fe_3O_4 with black color and relative volume of 2.1, $Fe(OH)_2$ with white color and relative volume of 3.8, $Fe(OH)_3$ with brown color and the relative volume of 4.2, and $Fe(OH)_3.3H_2$ with yellow color and the relative volume of 6.4, as shown in Fig.4b. These corrosion products can cause significant expansion, for the corrosion product of ferrous hydroxide, for example, the volume is about four times that of the consumed ferrite. This generates internal stress and, ultimately, causes cracking, delamination and spalling. In this paper, for Ø8 mm bars, the mass loss was 1.18%, 3.15%, 6.60%, while for Ø25 mm bars the mass corrosion rate was 0.99%, 2.10% and 4.46%. Hence, the mass loss of 8 mm bars was higher than 25 mm bars by 19%, 50% and 48%, respectively for 1, 3 and 5 years' exposure. In general, the mass loss of the rebar with

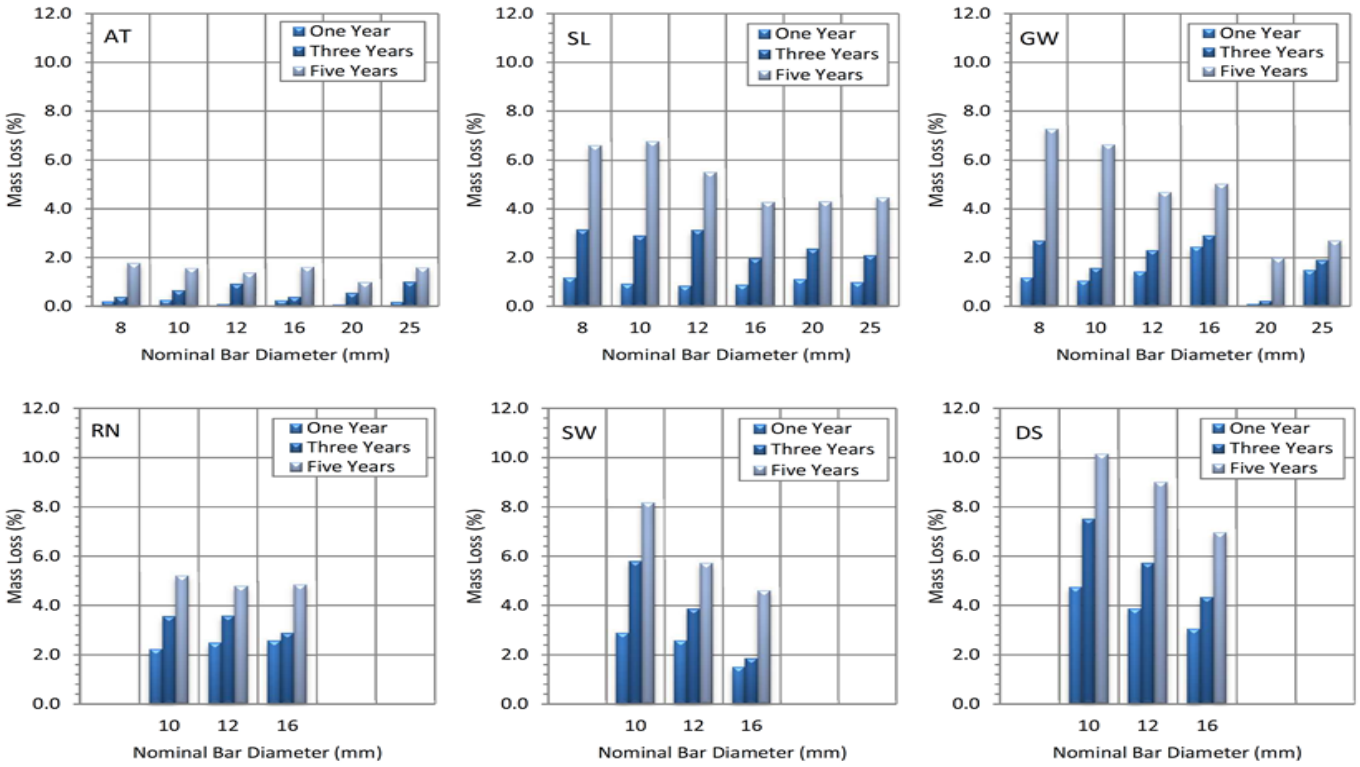

Fig.3. Mass loss of the reinforcing bars exposed to six different environments, AT (natural atmosphere), SL (buried in soil), GW (ground water), RN (rain water), SW (salty water), and DS (detergent solution)

Fig.4. (a) Specimens exposed to natural atmosphere for 5 years, (b) different corrosion products appeared in SL group.

larger diameter was less than that of smaller bars. In the ground water group of the specimens the mass corrosion rates after five years were 7.28%, 6.64%, 4.68%, 5.02%, 1.98% and 2.69%, for 8, 10, 12, 16, 20, and 25 mm bars, respectively. For specimens immersed in water, the corrosion process will be slow and may eventually stop when oxygen is limited. Since, very high humidity in conditions may reduce the diffusion of oxygen to the corrosion area, while a shortage of water in dry locations (such as AT group) reduces corrosion activity. The chloride, bicarbonate, and sulfate were the main possible causes of the corrosion progress, in addition to the dissolved gasses in water, in original form or during periodic stirring or agitating of the water, for instance, CO_2 in gas phase basically not a corrosive gas but in presence of water, water react with the gaseous CO_2 and forms carbonic acid and H^+ molecule that speed up the corrosion process. When the specimens removed from ground water buckets, they had covered with a layer of the corrosion products that partially prevents the direct contact of the water with the base material; the layer thickness was 3 mm approximately, as shown in Fig.5a.

Rain water can have a direct contact with the reinforcing bars through formation of the structural cracks or concrete degradation, or through the prestressing ducts to the un-grouted bare strands, or unfilled structural joints in segmental structures (Ahmed & Aziz, 2019). In this study, when the bars were submerged in rain water, the corrosion mass loss was 2.2- 2.6%, 2.9-3.6% and 4.8-5.2%, for 1, 3 and 5 years, respectively. When transferring the ratio to the loss per year, the average ratios became 2.4, 1.1 and 1.0%/year, which is proofing that the relation is not linear, and the first year of exposure was more aggressive than the upcoming years. The reinforcing bars of this group were covered by a layer of the corrosion products which was mostly ferric hydroxide ($Fe(OH)_3$), that the corrosion concentration were eventually caused by a pitting corrosion Fig.5b.

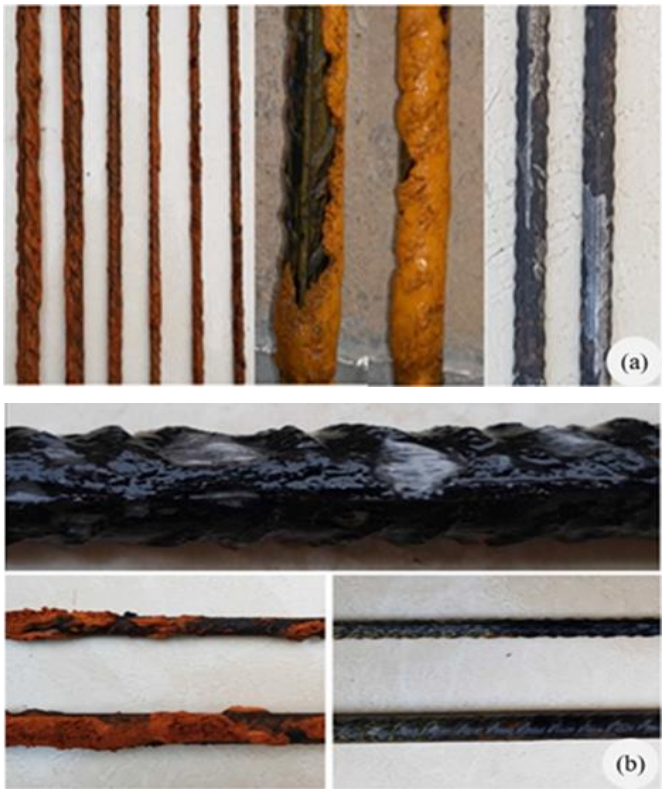

Fig.5. (a) specimens immersed in ground water for 5 years, (b) corrosion products and pit corrosion for specimens immersed in rain water

Based on pH value of 6.7, the rain water was acidic. As the acid concentrations were increased, the corrosion rates also increased. Ahmad (2003) stated that for pH values below 7.0, catastrophic corrosion occurs. This owed primarily to hydrogen ions, the active ions in acids. The corrosion of metals in acidic solution is cathode controlled by the hydrogen evolution reaction. Because it can scrub off the mechanically weak iron sulfate film, which is the only thing protecting the steel from the attack. A high chloride concentration of 4.68% assisted in activating a more aggressive environment relatively (Hay et al. 2019),

therefore the mass loss of the specimens immersed in the salty water was generally higher than the previous groups. It was known that when the concentration of chloride ions in the vicinity of steel bars exceeded to a certain threshold value, the protective film around the steel bars became unstable and its protection will be broken down, leading to a state of active steel corrosion. For 10, 12 and 16 mm bars, the mass loss was 1.5-2.9% in one year and was increased to 1.9-5.8% after 3 years to reach 4.6-8.2% in five years. The one-year mass loss was 2.2%, 1.3%, 1.3% based on the average of one, three and five years, respectively. Hence, it can be concluded that increasing in the corrosion rate was higher in the first year, however, later it might increase linearly. On the other side, the mass loss of the salty water group had a good relation with the bar diameters, since in all stages, the smaller specimens exhibited a higher mass loss than the greater bars.

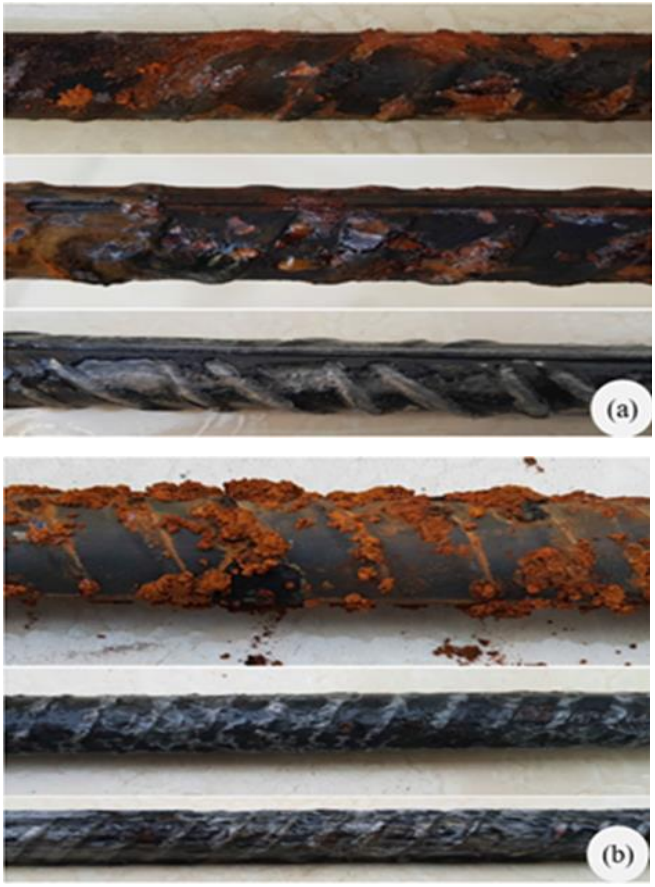

Fig.6. corrosion of the specimens after 5 years of exposure (a) immersed in salty water (b) detergent solution.

During the corrosion evolution, the smooth part of the rebar was less attacked relatively; however, bar deformations were severely attacked by high chloride concentration in the surrounding environment, as shown in Fig.6a. The rebar immersed in the detergent solution exhibited the highest mass loss among other tested environments. The corrosion rates of 3.1-4.8%, 4.3-7.5% and 7.0-10.2% were recorded for 1, 3 and 5 years, respectively. Based on the pH value of 9.8, the detergent solution was an alkaline environment containing carbonate, bicarbonate and sulfate ions. The solution was aggressive to the rebar corrosion, as shown in Fig.6b. The relation between mass loss/exposure period/bar diameter, is shown in Fig.7, it can be noted that the rates of increase in the corrosion per year are 1.35, 1.28 and 0.97, respectively for 10, 12 and 16 mm bars. In other words, the corrosion rates were 39% and 32% higher, respectively for 10 and 12 mm bars, compared to the 16 mm specimen. Larger cavities were observed on the surface of 12 mm rebar than of Ø16 rebar, which is consistent with the results reported by Zhang et al. (2014).

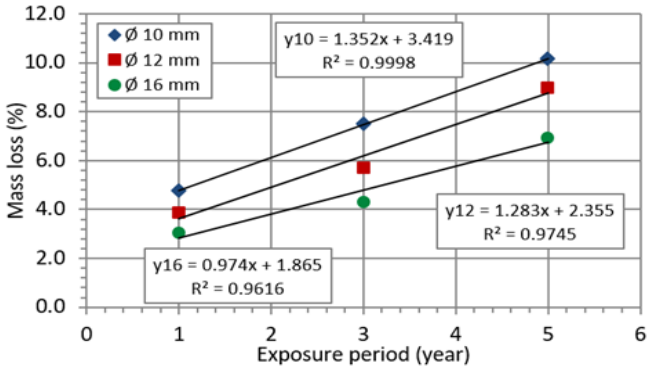

Fig.7. Mass loss – exposure period – bar diameter relationship for specimens immersed in detergent solution

One phenomenon that worth noting is, for reinforcing bars exposed to different environment for one year, the small cavities appeared at the skin of the ribs and deformation, shown in Fig.8. The deterioration certainly has influence on the mass loss, while it is actually not as effective as those in the smooth region of the rebar. Because it has been noted that the steel bar is not likely to fail over the deformations. Another important matter is the distribution of the corrosion along the rebar. For specimens embedded in concrete (Fig.9a), most researchers were referring the phenomenon to the local deterioration in the concrete cover or cracking of the concrete specimens due to various stresses (loading, thermal, etc.), however, in this study the bare bars also have similar pattern of corrosion along the longitudinal axis of the specimens, as shown in Fig.9b. Hence, in addition to the reasons explored for embedded rebar in concrete, more reason behind this non-uniform type of corrosion could be

the nature of chloride attack itself, or the surface treatment of the rebar during production. In un-cracked concrete the two attacks act completely different: carbonation phenomena involve equally large structural areas, leading to a uniform dissolution of steel; chloride ions instead destroy the passive layer locally. Hence, chloride attack is extremely dangerous, due to its localized and non-uniform nature (Finozzi et al. 2018; Zhang et al. 2020).

Fig.8. Cavities and deterioration on the ribs and deformations

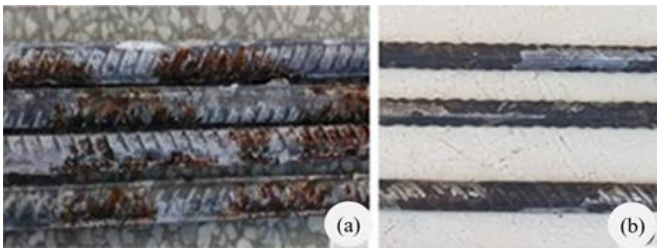

Fig.9. Intermittent corrosion along steel bars (a) specimens embedded in concrete (Lu et al. 2016), (b) bare bars immersed in ground water, current study

3.2 Reduction in the strength

In this study, the average reduced cross sections of the corroded bars were used for calculating the yield and ultimate strength. The reductions in ultimate load capacity of the six groups were shown in Fig.10, and the yield strength reductions were not plotted as they were mostly similar to those of ultimate strength. The strength loss is presented in Table 5 with respect to the exposure period of 1, 3 and 5 years. As expected, there was a significant increasing in the losing ratio of both strengths (yield and maximum) with respect to that of un-corroded steel bars due to various causes. Previous studies already reported a decreasing behavior of the elastic and ultimate strengths of corroded bars; however, in those studies mostly the accelerated tests were conducted, which might be exhibiting technical differences in the test methods, comparing to that used in this study. In all investigated conditions, two facts can be clearly observed. The first one is that, the strength loss was increased compared to its previous exposure period, except of the ultimate strength of one and three years for 16 mm bar of RN environment in Fig.10 that both resulted in 5% of the loss; which may refer to the stress concentration on the pits. The second fact is that the smaller bars were more likely to loss a higher strength ratio than the larger rebar. This has been proven by other authors (Huang 2014); that at the corrosion level of 5%, the reduction in the yield strength was 6.2 and 5.5%, and in the ultimate strength was 7.3 and 4.6% for 10 and 19 mm bars, respectively.

In aggressive environments when corrosion might cause losing of one-quarter of the tensile strength, reduction in ultimate strength could be really problematic for reinforced concrete structures. RC structures are generally designed based on the yield strength, and the ratio of yield/ultimate strength in this study was 0.68-0.86 (in ASTM A615 it is 0.68, 0.75 and 0.76, respectively for grades 420, 520 and 550). Thus, when the ultimate strength reduced by 14-32%, it falls below the yield strength, and eventually results in failure or collapse of the structures. For the test results shown in Fig.10, seven (8.6%) of the specimens exceeded that limit when the ultimate strength falls below the original yield strength. The specimens were: in SL group: Ø8 at 3 years (ultimate strength loss = 14.0% > 13.7% the limit) and at 5 years (17.1% > 13.7%); in GW group: Ø8 at 3 years (17.3% > 13.7%) and 5 years (20.4% > 13.7%); in SW group: Ø10 at 5 years (19.1% > 15.9%); in DS group: Ø10 at 5 years (19.1% > 15.9%) and Ø12 at 5 years (19.7% > 16.8%). The ultimate strength losses for the AT specimens were 0.2-2.0%, 0.5-2.7% and 0.8-10.1% for 1, 3 and 5 years, respectively. The maximum loss of 10.1% was recorded for Ø10 and the minimum loss was 0.2% for Ø12 and Ø25 after one-year of exposure, in which, a part of the loss might refer to the tolerance that already exist for un-corroded bars from same source when considering the average of three specimens. The buried specimens in the soil exhibited the losses of 1.2-7.6%, 4.1-14.0% and 6.9-17.1%, respectively for 1, 3 and 5 years. A systematic relationship between the bar diameters and the exposure period can be found for this group. The ground water had a large influence in reduction of the ultimate strength of Ø8 by decreasing 20.4% at 5 years, but the corresponding value for Ø25 was only 3.9%. The RN specimens had the reduction in ultimate strength of 3.8-5.0%, 5.0-10.2% and 6.2-13.8%, respectively for the three mentioned periods, while the SW group results were significantly higher and exhibited the loss of 2.0-6.2%, 7.4-12.9% and 10.1-19.1%, at 1, 3 and 5 years, respectively. The most destructive reductions were recorded for the DS group, in which the

reductions were 6.4%, 13.9% and 24.8% for Ø10, 5.6%, 10.8% and 19.7% for Ø12, and 4.4%, 11.8% and 18.4% for Ø16, for the three exposure durations, respectively. The losses in the first year were quite similar or even lower than those of SL and GW specimens; however, the detergent solution was causing corrosion pits in the advanced ages, and causing the local weakening of the bar cross sections, which was eventually resulting in the higher reduction (25%). The results recorded in this section were consistent with those reported by Apostolopolous et al. (2013) as they got, the ultimate strength reductions of 3.1%, 10.4% and 23.1%, for the mass loss of 1.3%, 5.2% and 13.6% respectively.

3.3 Reduction in fracture strain

Fracture strain is the ratio between increased length and the initial length, after breakage of the tested specimen. In construction practice and design, the ultimate strain considered as an important parameter to ensure rebar ductility, by which integrity of the reinforced structures. Standard specifications had limited the minimum ultimate strain, for instance ASTM A615, have minimum limits of 6-12%, according to bar diameter and strength grades. Fig.11 depicts the loss in fracture strain of all specimens exposed to the six different environmental conditions.

The AT group exhibited the strain reductions of 0.0-0.6%, 0.0-4.1% and 0.6-7.7% at 1, 3 and 5 years. These results were compatible to the reductions in the yield and ultimate strength, even the mass loss. In the SL specimens, a good relation between the strain reduction and the exposure period can be determined; however, it seems that the strain reduction is not strongly related to the bar diameter, since the maximum loss of 18.0 % was recorded for Ø12, followed by Ø8 with 12.0% and Ø16 with 11.3%. For the immersed specimens in GW, the losses were 2.3-17.8%, 4.0-21.5% and 6.8-26.7%, respectively for 1, 3, and 5 years. The maximum strain reduction of 26.7% was again recorded for Ø12, whereas, Ø25 showed the lowest value. The fracture strain of RN specimens was reduced by 5.1-9.2%, 13.6-16.5% and 16.3-24.8% respectively for the three durations. Both (strain reduction-exposure period) and (strain reduction-bar diameter) relations were more regular and systematic for SW specimens; which had the five year reduced ultimate strain of 22.0% 19.8% 18.6%, respectively for 10, 12 and 16 mm bars. The detergent solution had caused the strain reduction of 1.7-6.4%, 10.2-19.3% and 20.3-26.7%, respectively for 1, 3 and 5 years of exposure; and the results were consistent with the losses in, mass, yield and ultimate strength. When comparing the DS-Ø10

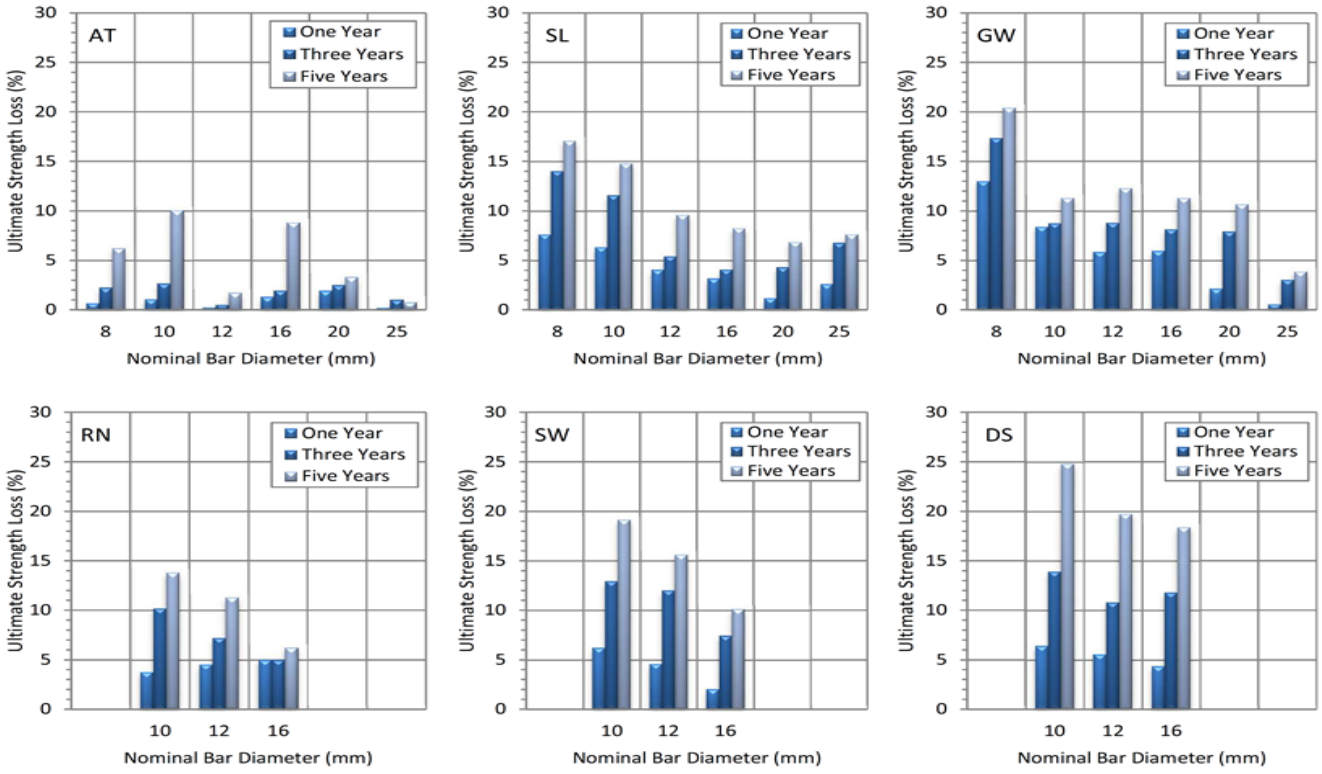

Fig.10. Reduction in ultimate strength of the reinforcing bars due to exposure to six different environments for 1, 3 and 5 year

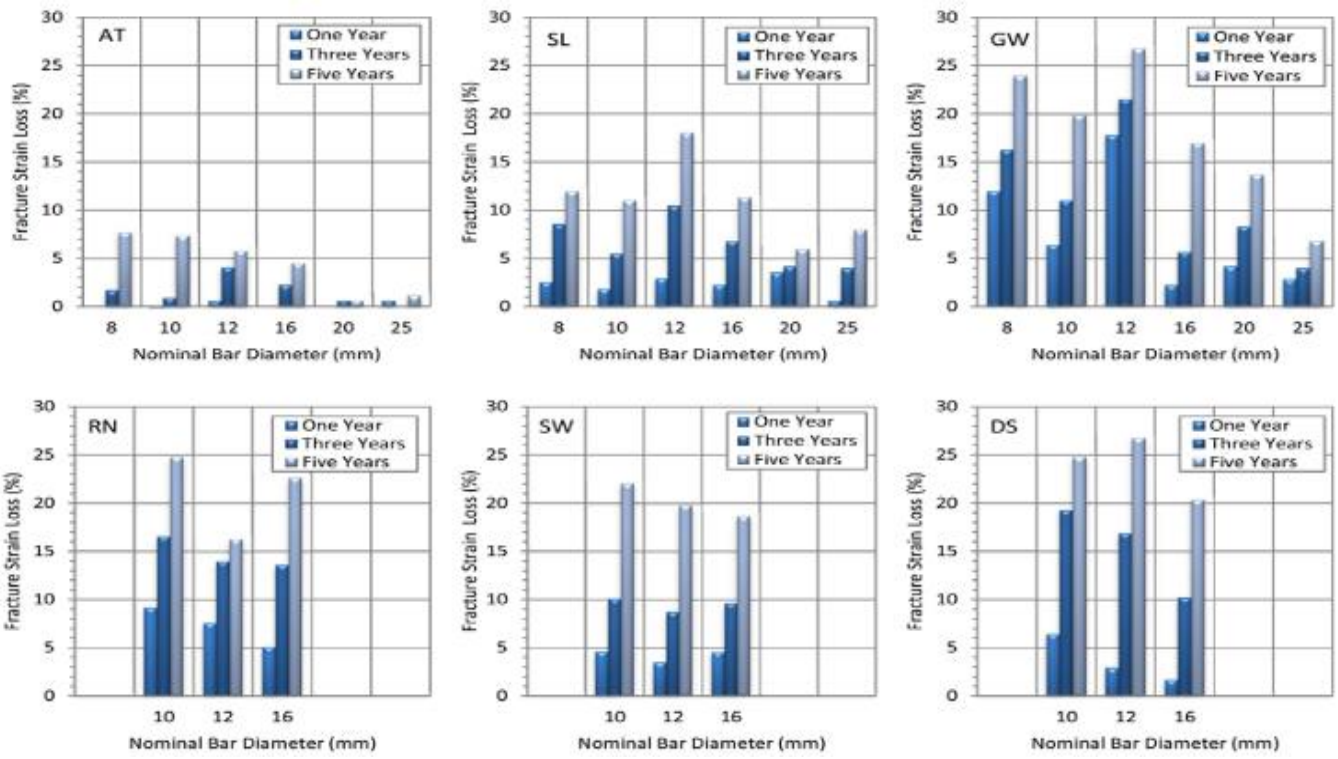

Fig.11. Reduction in fracture strain of the reinforcing bars due to exposure to six different environments for 1, 3 and 5 years

with 10.2% of the mass loss, and the reduction of 24.8% in the fracture strain, the results were close to those obtained by Zhu et al. (2017), that their reduction in the fracture strain was 24% for 10% of the mass loss. The strain reductions of 14-30% were recorded by Zhu for 6% of the mass loss, which were consistent also with that of Ø8 and Ø10 of the SL and GW groups. Almussalam (2001) results showed that the reduction in the ultimate strain for a Ø6 at the corrosion levels of 1.5 and 12.6% were 15.9 and 64.7%, respectively. Imperatore et al. (2017) revealed that the martensitic content was 25%, 30%, 33% and 38% for 8, 10, 12 and 18 mm rebar, respectively. This occurrence is explained from the physical point of view, that the martensitic layer is smaller in the lower diameter reinforcement; The thick martensitic cortex promotes the formation of cavities that quickly intercepts the weaker core. This level of the ductility reduction need more attention, and it is worth mentioning that for welded spliced rebar which already has lost 30-60% of it is ductility, the risk level is even higher (Ahmed, 2015).

3.4 Relationship of mass loss and the residual mechanical properties of the corroded bars

The relationships between mass loss and relative yield strength (the ratio of yield strength of a corroded to un-corroded specimen), relative ultimate strength, and relative fracture strain, were shown in Fig.12. Both strength and deformation capacities of the corroded specimens tended to decrease with increasing corrosion mass. However, the trend was less clear for the deformation capacity than for the strength. This is because the strength capacity was mainly related to the cross-sectional area; while, the deformation capacity was related to the cross-section area and also to the cross-section shape along the bar. This is consistent with that distribution of corrosion pits has a significant influence on the strain behavior of corroded steel bars, causing more scattered results. From the mass loss-mechanical property relations, it can be noted that yield, ultimate strength, and the fracture strain were decreased by 1.8%, 2.0% and 2.6% respectively, for each 1% of the mass loss. To quantify how residual mechanical properties of a corroded bar changes with the mass corrosion degree, the following empirical expression in Eq.2–4, can be used.

$$F_{yC} = (1 - 0.018M) \cdot F_y \quad (2)$$

$$F_{uC} = (1 - 0.020M) \cdot F_u \quad (3)$$

$$\varepsilon_{rC} = (1 - 0.026M) \cdot \varepsilon_r \quad (4)$$

Where:

F_{yC} is yield strength of the corroded rebar and F_y is yield strength of the corresponding un-corroded rebar (MPa), F_{uC} is ultimate strength of the corroded rebar (MPa) and F_u is ultimate strength of the corresponding un-corroded rebar (MPa), ε_{rC} is the fracture strain of the corroded rebar and ε_r is fracture strain of the corresponding un-corroded rebar, and M is the mass loss of the corroded bar (%).

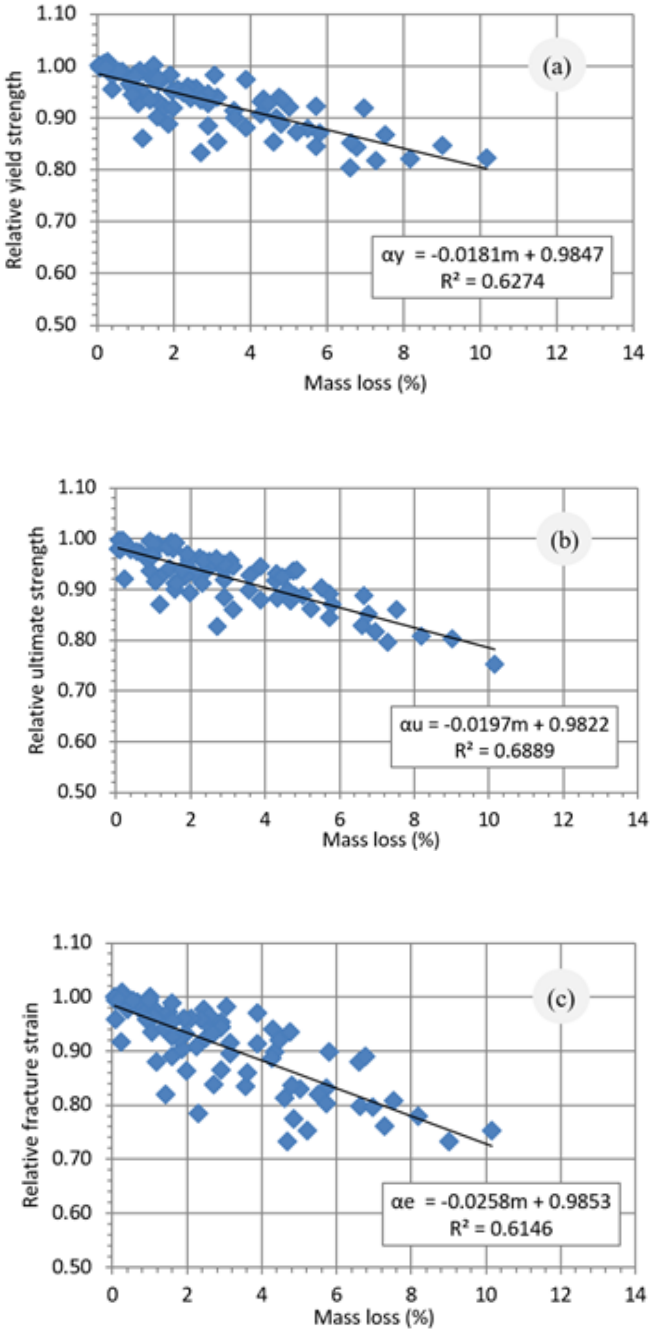

Fig.12. (a) Mass loss relationship with relative yield strength (corroded/uncorroded bar) (b) Mass loss vs relative ultimate strength (corroded/uncorroded bar), (c) Mass loss relationship with relative fracture strain (corroded/uncorroded bar)

Theoretically, the ordinate values in Eq.2 through Eq.4, must equals 1.0. The reduction coefficients (0.018, 0.020, and 0.026) in equations were representing the reduction rate of the tensile behaviors with increasing of the mass loss. In the other words, when the mass loss is 50%, the strength of the rebar could be considered as zero, since the remained half strength could not be ensured due to the pitting corrosion. What related to the fracture strain, the pits were more destructive, since the strength of the rebar is considered in the fracture section, while the corroded rebar might have different rates of the elongations at various sections along the specimen length. Regarding this fact, it is stated in by Zhu et al. (2017) that, the average cross-sectional area losses of the specimens were ranged from 4.4-25.2%, while the maximum cross-sectional loss could reach as high as 53.1%. Research revealed that the average strain of the bar is smaller than the local strain at the pit (Hanjari et al. 2011). Hence, the bar fails at an average strain smaller than the ultimate strain of the non-corroded bar and the average ductility of the bar is impaired. A very brittle behavior is expected when 50% of the cross-section of rebar is locally corroded. Therefore, the corrosion morphology should play an important role in the ultimate strain of the corroded reinforcement. Finozzi (2018) reported that, when strains are concentrated at the pit, the local strains of around 30% are detected in the damaged area, while the value of the overall strain is about 2.5%. This phenomenon intensifies in the final stages of the testing. The elongation of the pit was found to be 63.2% of the total bar elongation.

Previous research has also studied the relationship of the mass loss and the tensile behavior of rebar. The corresponding reduction coefficients proposed in this study (0.018, 0.020 and 0.026) were recorded by Ou et al. (2016) to be 0.0123, 0.0115, and 0.0125 for naturally corroded rebar; and, 0.0127, 0.0116 and 0.0281 for artificially corroded rebar, respectively for yield, ultimate and the fracture strain. Imeratore et al. (2017) values were 0.01510 and 0.01382, for the yield and ultimate strength formula (from experimental data), respectively, while for more collected data from literature, the reduction coefficient became 0.01996 and 0.01864, for yield and ultimate formula, respectively. Lu et al. (2016) reported 0.0195 and 0.0231 for yield and ultimate strength respectively. The reduction coefficients predicted in this study were considerably higher than those obtained by Ou et al., much closer to those predicted by Imperatore et al. from collected literature data, and comparable with those found by Lu et al.

4. CONCLUSIONS

This paper reports the experimental results of reinforcing bars exposed to six various environments with different corrosion mechanisms and aggressiveness degrees. The relationships between mechanical properties, exposure period, bar diameter, and the mass loss were determined and discussed. Based on the experimental evidences the following conclusions can be drawn:

1. When reinforcing bars are exposed to natural atmospheric conditions for 5 years, the mass loss was insignificant, and the reductions in the mechanical properties fell within the tolerance of the un-corroded reinforcing bars from the same source. The mass losses recorded for exposure of five years were within the range of 0.98 – 1.77%.
2. The specimens buried in soil (road subbase type) had the mass loss and mechanical properties similar to those immersed in the ground water, except of the fracture strain that the ground water results were slightly higher. The specimens buried in the soil for 5 years showed a mass loss of 4.3 – 6.8%; the ultimate strength loss of 6.9 – 17.1%; and reduction in fracture strain of 6.0 – 18.0%.
3. Among the four prepared liquid environments used for immersion of the specimens, the salty water and the detergent solution were more aggressive than the ground water and the rain water. For the salty water, the maximum reductions in the mass, ultimate strength and fracture strain were 8.2%, 19.1% and 22.0% in 5 years of exposure, and the maximum mass loss of the specimens exposed to salty water was 4.6 times higher than those exposed to natural atmosphere; while, for the detergent solution, the corresponding values were 10.2%, 24.8% and 26.7%, respectively.
4. The results revealed that the smaller bars were more likely to deteriorate in aggressive environments than the larger bars which can survive for a longer period with a higher reliability. Therefore, larger rebar should be chosen for structural design when the reduction of load bearing capacity caused by corrosion need to be considered. For the same environment (detergent solution) and exposure time (5 years), reduction in the ultimate strength for Ø12 was 34.8% higher than that of Ø16 mm.
5. In addition to the ductility considerations for corroded rebar in the aggressive environments, the designers should also be aware for the cases when the ultimate strength fell below the original yield strength used in design of RC structures. In this study, the ultimate strength of 8.6% of the corroded bars fell below the yield strength limit.
6. Yield and ultimate stresses measured in the monotonic tests were found strongly dependent on the corrosion degree; while, the ductility data seems to be more scattered, relatively. The corrosion morphology and the geometry of the residual cross-section played an important role in the ductility performance of the corroded rebar.
7. In the proposed equations, the losses in the ultimate strength, yielding strength, and fracture strain had followed a linear relationship with the mass-loss. The statistical analysis results showed that reductions in the yield strength, ultimate strength and fracture were 1.8%, 2.0% and 2.6% respectively for each 1% of mass-loss.

References

Ahmad S. 2003. Reinforcement corrosion in concrete structures, its monitoring and service life prediction-a review, Cement & Concrete Composites 25 (2003) 459-471.

Ahmed G.H. 2015. Mechanical properties of welded deformed reinforcing steel bars. ARO, The Scientific Journal of Koya University, Volume III, No 1(2015), Article ID: ARO.10059, Pp 28-39.

Almusallam A.A. 2001. Effect of degree of corrosion on the properties of reinforcing steel bars, Construction and Building Materials 15 (2001) 361-368.

Apostolopoulos C.A., Demis S., Papadakis V.G. 2013. Chloride-induced corrosion of steel reinforcement–Mechanical performance and pit depth analysis, Construction and Building Materials 38 (2013) 139-146.

ASTM A370-13. 2013. Standard test methods and definitions for mechanical testing of steel products, ASTM, West Conshohocken, Pennsylvania.

ASTM A615/A615M-09b. 2009. Deformed and plain

carbon-steel bars for concrete reinforcement, ASTM, West Conshohocken, Pennsylvania.

Babutskii A.I. 2010. Effect of electric current pulse treatment on the corrosion rate and strength of specimens made of 45 steel, Strength of Materials, 42(4), 2010, PP432-438.

Balestra C.E.T., Nakano A.Y., Savaris G., Junior R.A.M. 2019. Reinforcement corrosion risk of marine concrete structures evaluated through electrical resistivity: Proposal of parameters based on field structures, Ocean Engineering 187 (2019) 106167.

Bidi MA, Azadi M, Rassouli M. 2020. A new green inhibitor for lowering the corrosion rate of carbon steel in 1 M HCl solution: Hyalomma tick extract, Materials Today Communications (2020), doi: https://doi.org/10.1016/j.mtcomm.2020.100996 .

Diaz B., Guitian B., Novoa X.R., Perez M.C. 2020. The effect of chlorides on the corrosion behavior of weathered reinforcing bars, Electrochimica Acta 336 (2020) 135737.

Fernandez I., Bairan J.M., Mari A.R. 2015. Corrosion effects on the mechanical properties of reinforcing steel bars. Fatigue and σ–ε behavior, Construction and Building Materials 101 (2015) 772–783.

Finozzi I., Saetta A., Budelmann H. 2018. Structural response of reinforcing bars affected by pitting corrosion: experimental evaluation, Construction and Building Materials 192 (2018) 478–488.

G.H. Ahmed, O.Q. Aziz. 2019. Shear behavior of dry and epoxied joints in precast concrete segmental box girder bridges under direct shear loading. Engineering Structures 182 (2019) 89–100.

Gao Y., Zheng Y., Zhang J., Xu S., Zhou X., Zhang Y. 2019. Time-dependent corrosion process and non-uniform corrosion of reinforcement in RC flexural members in a tidal environment, Construction and Building Materials 213 (2019) 79–90.

Ghafur H. Ahmed, 2021. Influence of mixture proportions on fresh and mechanical properties of self-consolidating concrete. Polytechnic Journal. 2021. 11(2): 17-25.

Hanjari K.Z., Kettil P., Lundgren K. 2011. Analysis of mechanical behavior of corroded reinforced concrete structures. ACI Structural Journal, (2011) 108(5), 532-541.

Hay R., Ostertag C.P. 2019. Influence of transverse cracks and interfacial damage on corrosion of steel in concrete with and without fiber hybridization, Corrosion Science 153 (2019) 213–224. https://doi.org/10.1016/j.corsci.2019.03.020 .

Huang C.H. 2014. Effects of Rust and Scale of Reinforcing Bars on the Bond Performance of Reinforcement Concrete, J. Mater. Civ. Eng., 2014, 26(4): 576-581.

Imperatore S., Rinaldi Z., Drago C. 2017. Degradation relationships for the mechanical properties of corroded steel rebars, Construction and Building Materials 148 (2017) 219-230.

Lu C., Yuan S., Cheng P., Liu R. 2016. Mechanical properties of corroded steel bars in pre-cracked concrete suffering from chloride attack, Construction and Building Materials 123 (2016) 649–660.

Miao C.Q., Zhuang M.L., Dong B. 2019. Stress corrosion of bridge cable wire by the response surface method, Strength of Materials, 2019, 51(4), 646-652.

Ou Y.C., Y Susanto.T.T., Roh H. 2016. Tensile behavior of naturally and artificially corroded steel bars, Constr. Build. Mater.103 (2016) 93–104.

Tittarelli F., Mobilia A., Giosue C., Belli A., Bellezze T. 2018. Corrosion behavior of bare and galvanized steel in geopolymer and Ordinary Portland Cement based mortars with the same strength class exposed to chlorides, Corrosion Science (2018), https://doi.org/10.1016/j.corsci.2018.02.014 .

Uthaman S., George R.P., Vishwakarma V., Harilal M., Philip J. 2019. Enhanced seawater corrosion resistance of reinforcement in nanophase modified fly ash concrete, Construction and Building Materials 221 (2019) 232–243.

Wang X., Nguyen M., Stewart M.G., Syme M., Leitch A. 2010. Analysis of climate change impacts on the deterioration of concrete infrastructure–Part.1: Mechanisms, practices, modelling and simulations–A review, published by CSIRO, Canberra, (2010), ISBN 9780 4310365 8.

Wu Q.L., Yu H.F. 2019. Rebar corrosion rate estimation of reinforced concrete components exposed to marine environment, Strength of Materials, 51(4), 653-659.

Zhang W., Francois R., Yu L. 2020. Influence of load-induced cracks coupled or not with top-casting-induced defects on the corrosion of the longitudinal tensile reinforcement of naturally corroded beams exposed to chloride environment under sustained loading, Cem. Con. R. 129 (2020) 105972.

Zhang W., Zhou B., Gu X., Dai H. 2014. Probability distribution model for cross-sectional area of corroded reinforcing steel bars, Journal of Materials in Civil Engineering, 2014, 26(5): 822-832.

Zhu W., Francois R., Poon C.S., Dai J.G. 2017. Influences of corrosion degree and corrosion morphology on the ductility of steel reinforcement, Construction and Building Materials.

.